



Article

# Quantitative Immunomorphological Analysis of Heat Shock Proteins in Thyroid Follicular Adenoma and Carcinoma Tissues Reveals Their Potential for Differential Diagnosis and Points to a Role in Carcinogenesis

Alessandro Pitruzzella <sup>1</sup>, Letizia Paladino <sup>1</sup>, Alessandra Maria Vitale <sup>1</sup>, Stefania Martorana <sup>2</sup>, Calogero Cipolla <sup>2</sup>, Giuseppa Graceffa <sup>2</sup>, Daniela Cabibi <sup>3</sup>, Sabrina David <sup>1</sup>, Alberto Fucarino <sup>1</sup>, Fabio Bucchieri <sup>1</sup>, Francesco Cappello <sup>1,4</sup>, Everly Conway de Macario <sup>4,5</sup>, Alberto JL Macario <sup>4,5</sup>  and Francesca Rappa <sup>1,\*</sup> 

<sup>1</sup> Department of Biomedicine, Neuroscience and Advanced Diagnostics (BIND), Institute of Human Anatomy and Histology, University of Palermo, 90127 Palermo, Italy; alessandro.pitruzzella@unipa.it (A.P.); letizia.paladino@unipa.it (L.P.); alessandra.vitale92@gmail.com (A.M.V.); sabrina.david@unipa.it (S.D.); alberto.fucarino@unipa.it (A.F.); fabio.bucchieri@unipa.it (F.B.); francesco.cappello@unipa.it (F.C.)

<sup>2</sup> Department of Surgical Oncological and Oral Sciences, University of Palermo, 90127 Palermo, Italy; stefania.martorana@unipa.it (S.M.); calogero.cipolla@unipa.it (C.C.); giuseppa.graceffa@unipa.it (G.G.)

<sup>3</sup> Department “G. D’Alessandro”, Pathology Institute, University of Palermo, 90127 Palermo, Italy; daniela.cabibi@unipa.it

<sup>4</sup> Euro-Mediterranean Institute of Science and Technology (IEMEST), 90100 Palermo, Italy; econwaydemacario@som.umaryland.edu (E.C.deM.); AJLMacario@som.umaryland.edu (A.J.L.M.)

<sup>5</sup> Department of Microbiology and Immunology, School of Medicine, University of Maryland at Baltimore-Institute of Marine and Environmental Technology (IMET), Baltimore, MD 21202, USA

\* Correspondence: francyrappa@hotmail.com

Received: 17 September 2019; Accepted: 11 October 2019; Published: 15 October 2019



**Abstract:** Hsp27, Hsp60, Hsp70, and Hsp90 are chaperones that play a crucial role in cellular homeostasis and differentiation, but they may be implicated in carcinogenesis. Follicular neoplasms of the thyroid include follicular adenoma and follicular carcinoma. The former is a very frequent benign encapsulated nodule, whereas the other is a nodule that infiltrates the capsule, blood vessels and the adjacent parenchyma, with a tendency to metastasize. The main objective was to assess the potential of the Hsps in differential diagnosis and carcinogenesis. We quantified by immunohistochemistry Hsp27, Hsp60, Hsp70, and Hsp90 on thin sections of human thyroid tissue with follicular adenoma or follicular carcinoma, comparing the tumor with the adjacent peritumoral tissue. Hsp60, Hsp70, and Hsp90 were increased in follicular carcinoma compared to follicular adenoma, while Hsp27 showed no difference. Histochemical quantification of Hsp60, Hsp70, and Hsp90 allows diagnostic distinction between follicular adenoma and carcinoma, and between tumor and adjacent non-tumoral tissue. The quantitative variations of these chaperones in follicular carcinoma suggest their involvement in tumorigenesis, for instance in processes such as invasion of thyroid parenchyma and metastasization.

**Keywords:** Hsp27; Hsp60; Hsp70; Hsp90; molecular chaperone; chaperonopathies; thyroid; follicular adenoma; follicular carcinoma; differential diagnosis; carcinogenesis

## 1. Introduction

Thyroid tumors are the most frequent endocrine malignancies and their incidence is steadily increasing [1]. They are divided into epithelial and non-epithelial tumors. Follicular neoplasms of the

thyroid gland include benign follicular adenoma (FA) and follicular carcinoma (FC) [2]. FA is the most common benign thyroid tumor and occurs in follicular cells. Macroscopically, it may appear as a single nodule, whose diameter can vary from a few millimetres to a few centimetres, surrounded by a single capsule. Microscopically, it is characterized by the proliferation of many follicles surrounded by a capsule and, depending on their size the adenomas can be sorted into normofollicular, microfollicular, macrofollicular, and solid-trabecular.

Among thyroid carcinomas, FC is the second most common epithelial tumor after papillary carcinoma, occurring late in life, with the fifth and sixth decades being the most affected, and is more aggressive than papillary carcinoma [3]. Macroscopically it appears as a thyroid nodule of variable diameter and may or may not possess a capsule. Microscopically, FC consists of a proliferation of follicles, similarly to FA, but the neoplastic follicles invade the tumor capsule when present, penetrating into blood vessels and/or the adjacent normal thyroid tissue, a feature that can only be appreciated with histological but not with cytological techniques [4].

Immunohistochemical analysis does not usually allow the differentiation between benign and malignant lesions and, as a consequence, the majority of patients with these lesions are referred to surgery without a precise diagnosis. For this reason, it is necessary to improve the preoperative diagnosis also because no clinical, radiological, or laboratory test currently available is sufficiently sensitive and specific to distinguish benign from malignant follicular lesions detected by fine-needle aspiration [5].

Molecular chaperones are the main components of the chaperoning system with canonical and non-canonical functions [6,7]. The former functions pertain to maintenance of protein homeostasis and include assisting in the: folding of nascent polypeptides as soon as they emerge from the ribosome and until they reach their native and biologically active tridimensional structure; prevention of protein misfolding and aggregation; translocation of proteins from one cell compartment to another; and driving damaged or unnecessary proteins toward degradation [8–12].

Many chaperones are heat shock proteins (Hsp) but although not all Hsp are chaperones the terms molecular chaperone (or chaperone in short) and Hsp are used as synonyms. Chaperones are classified according to molecular weight [7] and designated variously, which causes confusion, and because of this, attempts at nomenclature standardization have been made [13].

Although chaperones are considered essentially cytoprotective, it is now known that they can also be pathogenic if abnormal in structure, or location, or quantity, causing diseases named chaperonopathies, including several types of cancer [7,14].

Some chaperones are increased in various cancers with the magnitude of the increase being closely associated with prognosis and with resistance to anticancer therapy, the former being worse and the latter being higher as the chaperones increase is bigger [15,16].

There are few data in the literature on the role of Hsp in thyroid cancer, for example Hsp27 was increased in anaplastic carcinoma [17], and in papillary carcinoma, in which it was induced by 17  $\beta$ -estradiol, which facilitates proliferation and confers resistance to apoptosis [18]. In this study, we performed immunomorphological analysis on samples of FA and FC to evaluate, for the first time to our knowledge, the tissue levels of Hsp27, Hsp60, Hsp70, and Hsp90. We focused on these chaperones based on the fact that they are implicated in chaperonopathies, including carcinogenesis [15,19].

## 2. Materials and Methods

### 2.1. Sample Collection

Formalin-fixed and paraffin-embedded thyroid tissue of human FA and FC (10 samples for each group) were retrieved from the archives of the Department of Human Pathology of the University of Palermo to perform immunohistochemical assays for Hsp27, Hsp60, Hsp70, and Hsp90. These samples were from patients who had undergone thyroidectomy surgery in the Department of Surgical, Oncological and Oral Sciences at the University of Palermo (Table 1). The experiments related to this

study were conducted as part of the study project approved by the Ethics Committee of University Hospital AUOP Paolo Giaccone of Palermo (N° 05/2017 of 05/10/2017).

**Table 1.** Patient demographics and tumor characteristics.

Sex	Age (yrs)*	Localization	Thyroid Weight (g)	Nodules Size (mm)	
<b>FOLLICULAR ADENOMA</b>					
M	27	Right lobe	35	17	
F	39	Right lobe	15	28	
F	69	Left lobe	30	24	
M	46	Right lobe	35	32	
F	73	Left lobe	120	30	
F	55	Left lobe	20	20	
F	67	Right lobe	40	22	
M	35	Left lobe	55	38	
F	29	Isthmus	60	42	
F	48	Right lobe	70	15	
<b>FOLLICULAR CARCINOMA</b>					<b>Stage (AJCC/TNM)</b>
F	41	Left lobe	45	25	I
F	29	Right lobe	35	30	I
M	62	Right lobe	80	35	I
F	51	Right lobe	50	40	I
F	48	Isthmus	20	28	I
F	39	Left lobe	25	25	I
M	67	Right lobe	45	38	II
F	57	Right lobe	60	22	II
F	29	Left lobe	25	19	I
F	61	Right lobe	30	41	I

\*Abbreviations. Yrs, years; M, male; F, female; AJCC, American Joint Committee on Cancer; TNM, Tumor-Nodes-Metastasis.

## 2.2. Immunohistochemistry

Immunohistochemical experiments were performed on 5-micron thick sections of paraffin-embedded tissue, obtained with a cutting microtome. The slides were dewaxed in xylene for 30 min at 60 °C and rehydrated, at 22 °C, by sequential immersion in a graded series of alcohols and transferred into distilled water for 5 min. Then, the sections were incubated for 8 min in Sodium Citrate Buffer (pH 6) at 95 °C for antigen unmasking and immersed for 8 min in acetone at −20 °C to prevent the detachment of the sections from the slide. After a wash of sections with PBS (Phosphate Buffered Saline pH 7.4) at 22 °C for 5 min, the experiments for Hsp60, Hsp70, and Hsp90 were performed applying a streptavidin–biotin complex method, using Histostain<sup>®</sup>-Plus 3rd Gen IHC Detection Kit (Life Technologies, Frederick, MD, USA; Cat. No. 85–9073). Therefore, the sections were treated for 5 min with Peroxidase Quenching Solution (reagent A of Histostain<sup>®</sup>-Plus 3rd Gen IHC Detection Kit, Life Technologies) to inhibit endogenous peroxidase activity, and after another wash with PBS at 22 °C for 5 min, were treated with blocking solution (reagent B of Histostain<sup>®</sup>-Plus 3rd Gen IHC Detection Kit, Life Technologies) for 10 min to block non-specific antigenic sites. Subsequently, the sections were incubated overnight at 22 °C, with a primary antibody against human Hsp60 (rabbit anti-Hsp60 polyclonal antibody, Santa Cruz Biotechnology, Inc., Santa Cruz, CA, USA, cat. N°: sc-13966, dilution 1:300), human Hsp70 (mouse anti-Hsp70 monoclonal antibody, clone W27, Santa Cruz Biotechnology, Inc, Santa Cruz, CA, USA, cat. N°: sc-24, dilution 1:200) and human Hsp90 (mouse anti-Hsp90 monoclonal antibody, clone F-8, Santa Cruz Biotechnology, Inc., Santa Cruz, CA, USA, cat. N°: sc-13119, dilution 1:200). Appropriate positive and negative (isotype) controls, were run concurrently. The following day, after a wash with PBS at 22 °C for 5 min, the sections were incubated with a universal

biotinylated secondary antibody (Biotinylated Secondary Antibody reagent C Histostain<sup>®</sup>-Plus 3rd Gen IHC Detection Kit, Life Technologies) for 10 min. After a subsequent washing with PBS for 5 min, the sections were incubated with streptavidin-peroxidase complex (Streptavidin-Peroxidase Conjugate reagent D Histostain<sup>®</sup>-Plus 3rd Gen IHC Detection Kit, Life Technologies) for 10 min, and following a further washing in PBS for 5 min, the slides were incubated in the dark for 5 min with the DAB chromogen (diaminobenzidine) (DAB chromogen reagents E1 and E2 Histostain<sup>®</sup>-Plus 3rd Gen IHC Detection Kit, Life Technologies). The experiments for Hsp27 were performed using an IHC goat kit (Cell & Tissue Staining Kit, R&D Systems, Inc., Minneapolis, MN, USA, Cat N° CTS008). Sections, after deparaffinization, were treated at 22 °C for 5 min with Peroxidase Blocking Reagent (Cell & Tissue Staining Kit, R&D Systems, Inc.) to inhibit endogenous peroxidase activity and after another wash with PBS for 5 min, with a Serum Blocking Reagent D (Cell & Tissue Staining Kit, R&D Systems, Inc.) for 15 min to block non-specific antigenic sites. Since the detection is based on the formation of Avidin-Biotin complex, the sections were treated with Avidin Blocking Reagent (Cell & Tissue Staining Kit, R&D Systems, Inc.) at 22 °C for 15 min. After a wash with PBS, the sections were incubated with Biotin Blocking Reagent for 15' (Cell & Tissue Staining Kit, R&D Systems, Inc.). After another wash with PBS, the sections were incubated at 22 °C overnight, with a primary antibody against human Hsp27 (goat anti-Hsp27 polyclonal antibody, Santa Cruz Biotechnology, Inc., Santa Cruz, CA, USA, cat. N°: sc-1048, dilution 1:150). For all samples, appropriate positive and negative (isotype) controls were run concurrently. So the samples were washed at 22 °C three times in PBS for 15 min/wash, and then the sections were incubated with Biotinylated Secondary Antibody (Cell & Tissue Staining Kit, R&D Systems, Inc.) for 40 min most often (the length of this incubation time varies depending on the thickness of the section). After that, the slides were washed three times in PBS for 15 min/wash. The high detection sensitivity of this method is obtained by using premium quality biotinylated secondary antibodies and High Sensitivity Streptavidin-conjugated HRP (HSS-HRP). HSS is a chemical analog of Streptavidin that interacts only with Biotin bound to secondary antibodies. The sections were incubated at 22 °C with HSS-HRP (Vial B, Cell & Tissue Staining Kit, R&D Systems, Inc.) for 30 min. For all samples, the visualization is based on enzymatic conversion of chromogenic substrates 3,3' Diaminobenzidine (DAB) into a colored precipitate (brown), by horseradish peroxidase (HRP) at the sites of antigen localization, after two subsequent washing with PBS for 2 min/wash, the slides were incubated in the dark for 5 min with the DAB chromogen (200 µL of DAB chromogen solution were required to cover tissue section on a single slide). Two drops of DAB Chromogen were added to 2 mL of DAB Chromogen Buffer (Cell & Tissue Staining Kit, R&D Systems, Inc.).

The nuclei were counterstained with hematoxylin (Hematoxylin aqueous formula, REF 05-06012/LN. Cat. S2020, Bio-Optica, Milano, Italy). Finally, the slides were mounted for observation with coverslips using a permanent mounting medium (Vecta Mount, H-5000, Vector Laboratories, Inc. Burlingame, CA, USA). The observation of the sections was carried out with an optical microscope (Leica DM 5000 B, Leica Microsystems Srl, Buccinasco (MI), Italy) connected to a digital camera (Leica DC 300F).

Two independent observers (F.C. and F.R) examined all specimens on two separate occasions and performed a quantitative analysis to quantify the percentage of epithelial cells positive for Hsp27, Hsp60, Hsp70, and Hsp90. All the observations were done at a magnification of 400× and the percentage of positive cells was calculated in a high-power field (HPF) and repeated for 10 HPF. The immunopositivity evaluation is expressed as average percentage of all immuno-quantifications performed in each case for each Hsp. Statistical analyses were carried out using the GraphPad Prism 4.0 package (GraphPad Inc., San Diego, CA, USA). One-way ANOVA analysis of variance with Bonferroni post-hoc multiple comparisons was used to detect significant statistical differences. All data are reported as the means ± SD, and the level of statistical significance was set at  $p \leq 0.05$ .

### 2.3. Results

The presence and levels of Hsp27, Hsp60, Hsp70 and, Hsp90 were determined in the tumor tissue itself and in the adjacent parenchyma (AP) of FA and FC. The immunopositivity for Hsp27 was observed in the cytoplasm and the nucleus in tumoral cells while only in the cytoplasm in the cells of the adjacent parenchyma. It was high in all specimens and it did not show significant quantitative differences between the specimens or tissue type: it was 73% in FA and 70% in its AP, and 68% in FC and 47% in its AP (Figure 1).

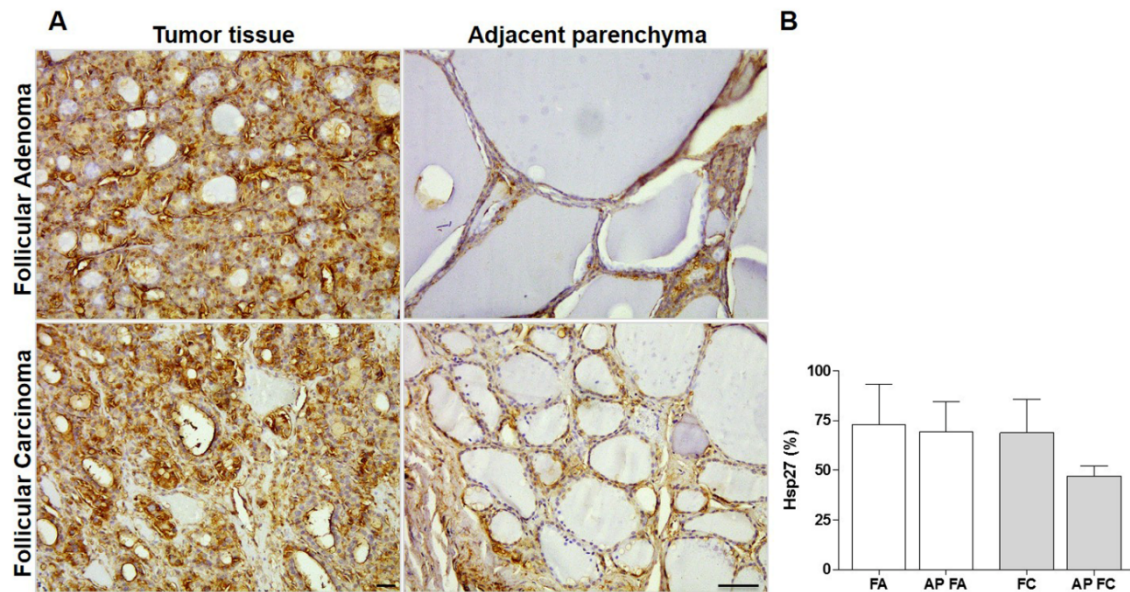


**Figure 1.** Hsp27 Immunohistochemistry. (A) Representative images of immunohistochemical results for Hsp27. Magnification 200×; scale bar 100  $\mu$ m. (B) The histogram shows statistical results for the immunohistochemical evaluation for Hsp27 in follicular adenoma (FA), adjacent parenchyma of follicular adenoma (AP FA), follicular carcinoma (FC) and adjacent parenchyma of follicular carcinoma (AP FC). Data are presented as mean +SD.

The Hsp60 tissue levels were 33% in FA and 7% in its AP with a significant difference ( $p \leq 0.01$ ), and in FC the immunopositivity was 74% and 6% in its AP with a significant difference ( $p \leq 0.001$ ). In the FA and FC epithelial cells, the immunopositivity was diffuse in the cytoplasm while in the epithelial cells of the AP was also in the cytoplasm but mild and granular. Statistical analysis also, showed a significant difference between FA and FC ( $p \leq 0.001$ ) (Figure 2).

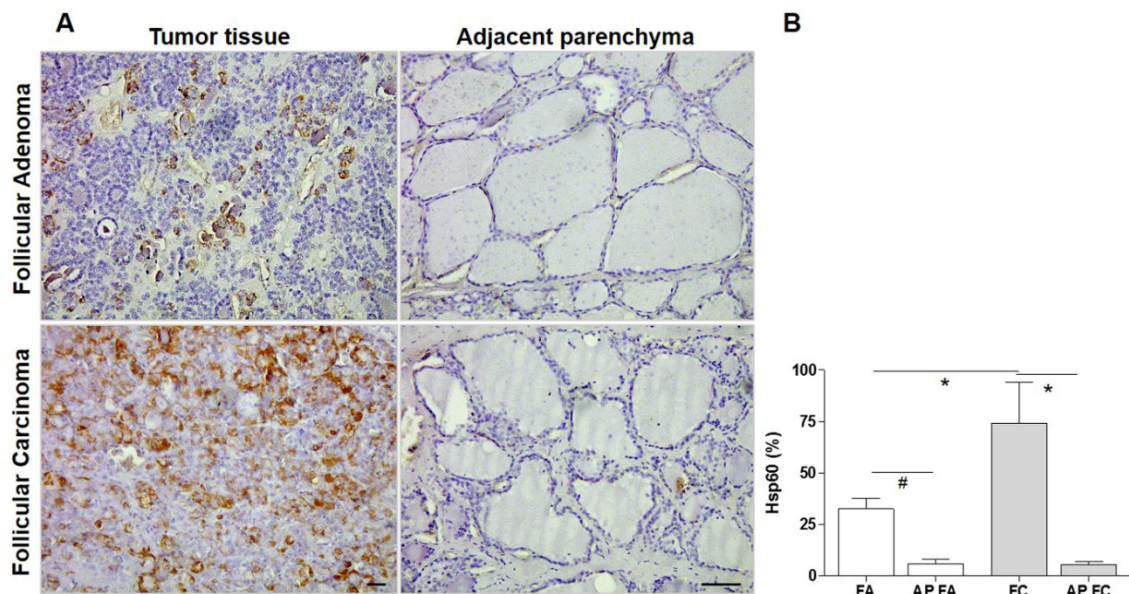


**Figure 2.** Hsp60 Immunohistochemistry. (A) Representative images of immunohistochemical results for Hsp60. Magnification 200X; scale bar 100  $\mu$ m. (B) The histogram shows statistical results for the immunohistochemical evaluation for Hsp60 in follicular adenoma (FA), adjacent parenchyma of follicular adenoma (AP FA), follicular carcinoma (FC) and adjacent parenchyma of follicular carcinoma (AP FC). Data are presented as the mean +SD. \*  $p \leq 0.0001$ , #  $p \leq 0.01$ .

The results for Hsp70 showed a positivity of 18% and 8% in FA and its AP, respectively, with no statistical difference, and of 55% and 7% in FC and its AP, respectively, with a statistical difference ( $p \leq 0.001$ ). The epithelial cells of FC showed a high cytoplasmic positivity while those of FA and the AP of both neoformations, showed a mild and pointed immunopositivity. Statistical analysis also showed a significant difference between FA and FC ( $p \leq 0.001$ ) (Figure 3).

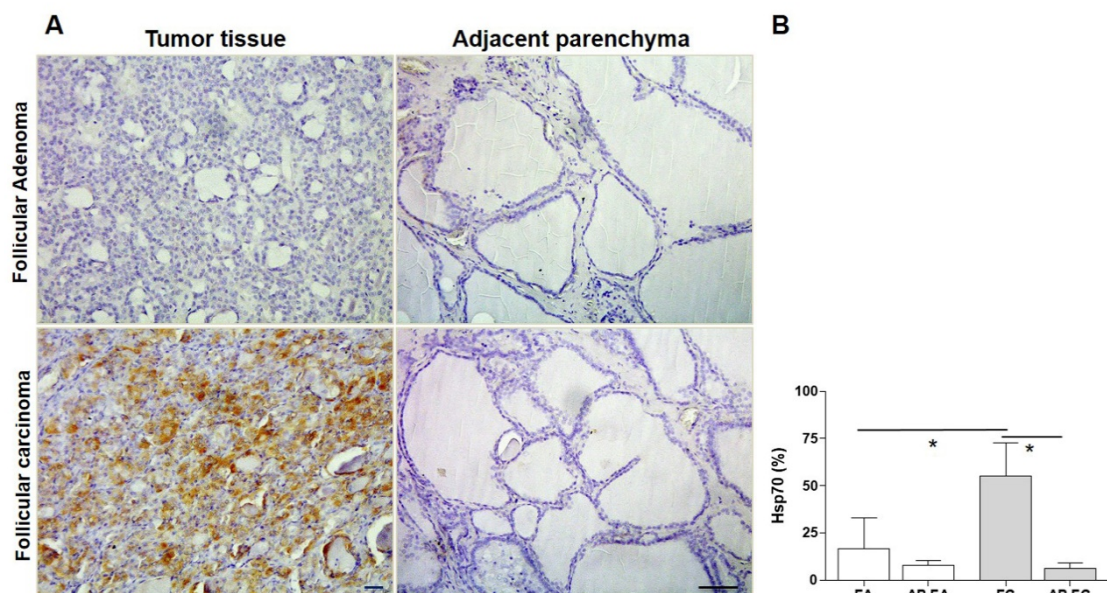


**Figure 3.** Hsp70 Immunohistochemistry. (A) Representative images of immunohistochemical results for Hsp70. Magnification 200 $\times$ ; scale bar 100  $\mu$ m. (B) The histogram shows statistical results for the immunohistochemical evaluation for Hsp70 in follicular adenoma (FA), adjacent parenchyma of follicular adenoma (AP FA), follicular carcinoma (FC) and adjacent parenchyma of follicular carcinoma (AP FC). Data are presented as the mean +SD. \*  $p \leq 0.0001$ .

The tissue levels of Hsp90 were 25% in FA and 15% in its AP, and were 56% in FC and 33% in its AP with no statistical difference. In all specimens the immunopositivity was cytoplasmic, intense in the FC and FA cells while mild in the cells of the AP. Statistical analysis also showed a significant difference between FA and FC ( $p \leq 0.05$ ) (Figure 4).

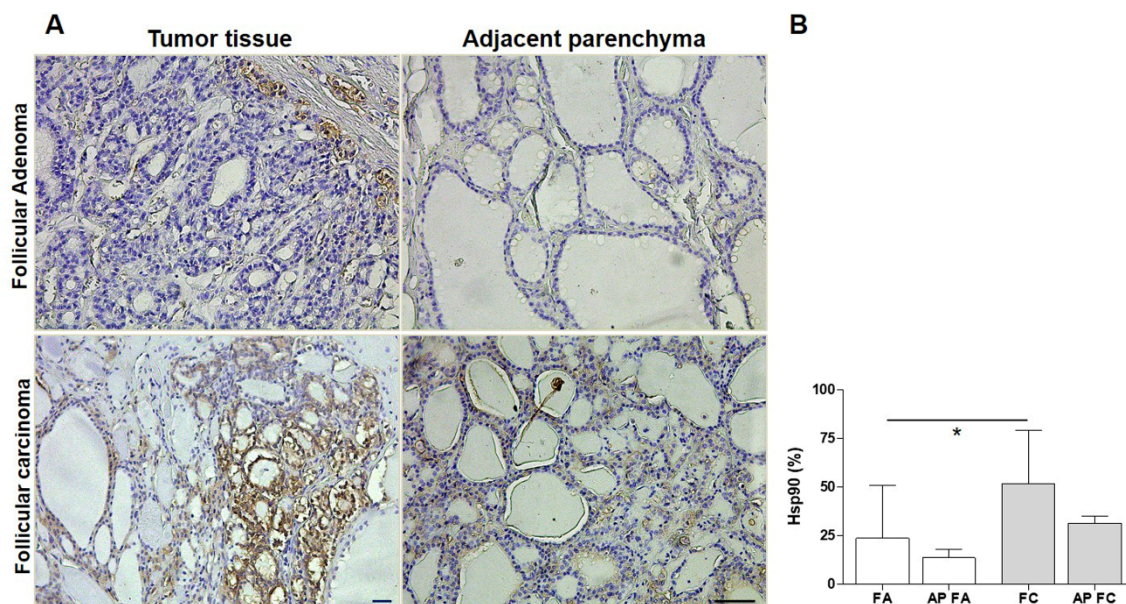


**Figure 4.** Hsp90 Immunohistochemistry: (A) Representative images of immunohistochemical results for Hsp90. Magnification 200 $\times$ ; scale bar 100  $\mu$ m. (B) The histogram shows statistical results for the immunohistochemical evaluation for Hsp90 in follicular adenoma (FA), adjacent parenchyma of follicular adenoma (AP FA), follicular carcinoma (FC) and adjacent parenchyma of follicular carcinoma (AP FC). Data are presented as the mean +SD. \*  $p < 0.05$ .

Our immunohistochemical observation was also dedicated to the evaluation of the intracellular localization of the Hsp immunopositivity. We observed an accumulation of Hsp60, Hsp70, and Hsp90 in the cytoplasm and of Hsp27 in the cytoplasm and in the nucleus.

### 3. Discussion

In this work, we studied the immunohistochemical levels of Hsp27, Hsp60, Hsp70, and Hsp90 in human thyroid tissue with follicular adenoma (FA) and follicular carcinoma (FC). FC is characterized by the ability to invade the tumor capsule when this is present and forcing its way inside blood vessels and in the adjacent normal thyroid tissue. This characteristic distinguishes FC from FA. In general, the pathological condition of cancer is characterized by an imbalance between cell proliferation and differentiation. A physiological balance between cell proliferation and differentiation is essential to ensure proper growth and development of multicellular organisms, and to maintain adult tissue and organ homeostasis. It is of fundamental interest in cancer pathology to understand the mechanisms underpinning the origin of the loss of cell differentiation capability and the induction of malignancy progression. Molecular chaperones play a key role in the maintenance of cellular and tissue homeostasis and in the regulation of organ remodelling [20–23]. However, when abnormal in structure and/or quantity and/or function, and/or location, chaperones can cause disease, the chaperonopathies [7,14], and numerous scientific reports showed their involvement in the pathogenesis and progression of various human neoplasms [15,19,24]. High tissue levels of Hsps are often associated with cancer progression and invasiveness, as shown by studies in which it was suggested that these proteins are augmented in some types of tumors with tendency to invade surrounding tissues and to spread to distant organs [19,25–27].

Hsp27 was initially characterized as a chaperone that facilitates the refolding of damaged proteins in response to heat shock. Further investigations revealed that Hsp27 also responds to oxidative and chemical stressors, mainly acting as an antioxidant and antiapoptotic agent. It was observed that an increase of Hsp27 levels is transiently induced at specific stages during development and cell differentiation and occurs concomitantly with the differentiation-associated decrease of cellular proliferation [28,29]. Other studies reported that Hsp27 is augmented in different types of tumors and its levels are directly associated with a more aggressive malignant behavior (cancer cell proliferation, invasiveness, and metastasis) and resistance to chemotherapy [30,31]. Furthermore, Hsp27 mediates endothelial cell mobility, improving angiogenesis [32].

The eukaryotic Hsp60 resides and works in the mitochondrial matrix where, together with its co-chaperonin Hsp10, drives the proper folding of proteins destined to the mitochondrial matrix. In addition to this intramitochondrial function, Hsp60 plays a role in other cellular processes beyond the mitochondrion, for instance in the cytosol, plasma-cell membrane, extracellular environment, and biological fluids) [33]. Hsp60 seems to be directly or indirectly involved in carcinogenesis in different organs, since its levels change during the carcinogenetic steps [15,24]. Hsp60 levels are increased in various tumors such as colorectal cancer, liver and uterine cervical cancers and its levels are correlated with cancer progression, which makes this chaperonin a useful biomarker indicating poor prognosis [34,35].

There are many reports of a strong association of Hsp70 with cancer development. For instance, it promotes carcinogenesis by acting as survival factor owing to its tumor-associated expression and anti-apoptotic effects [36]. Hsp70 abundance gives the neoplasm greater invasiveness [37].

Hsp90 is also augmented in various cancers, apparently playing important roles in cancer biology by regulating tumor growth, invasion, metastasis, angiogenesis, and apoptosis, and induces neoangiogenesis by stabilizing vascular endothelial growth factor and nitric oxide syntheses [38–40].

In light of what is available in the literature in the field of Hsp and cancer, very briefly summarized in the preceding paragraphs, we decided to evaluate the tissue levels of the four molecular chaperones discussed above, simultaneously, in samples of thyroid follicular neoplasms, about which there is little information. We also observed the localization of these Hsp in tumor cells to evaluate their possible localization change.

Hsp27 levels did not show significant quantitative differences between the groups studied. This result is in contrast with the data present in the literature on other types of tumors, which indicates that the thyroid tumors deserve detailed analysis to elucidate the basis for this unique feature regarding Hsp27. However, even if we did not find a quantitative difference, we observed a nuclear localization that, according to the data in the literature, would be linked to the phosphorylation of the chaperone [41].

Conversely, we observed a higher immunopositivity of Hsp60, Hsp70, and Hsp90 in FC compared to FA and their adjacent parenchyma. These data are in agreement with what has been published in the literature on other types of tumors. The increase of Hsp60 and Hsp70 in FC suggest its implication in carcinogenesis and in the progression of this tumor. Hsp60 and Hsp70 levels in FC were higher compared to adjacent parenchyma levels. In normal cells, Hsp 60 is detected in the mitochondria while in tumoral cells it is abundant in the cytoplasm. These data are interesting because both Hsps could be considered tumor tissue markers. Likewise, the higher levels of Hsp90 might indicate its implication in the process of FC invasion of surrounding tissue. This could be attributed to the known stabilizing effects of Hsp90 on matrix metalloproteinases, which would favor tumor infiltration and invasion [42,43].

In conclusion, our immunohistochemical data suggest an involvement of Hsp60, Hsp70, and Hsp90 in the mechanisms of carcinogenesis of thyroid follicular carcinoma. The immunomorphological observation showed a change in cellular localization of the Hsps studied. This pattern is found in various carcinogenic processes [19,24]. It is necessary to continue these studies to clarify the molecular mechanisms underlying the increase in tissue levels of these chaperones in this human cancer. In this regard, determination of chaperone-gene expression levels and elucidation of post-transcriptional



mechanisms that might be involved in augmenting the levels of the chaperones in thyroid tumors seem to be the most promising approaches toward finding points of attacks by anti-cancer agents.

**Author Contributions:** Conceptualization: C.C., F.C. and F.R.; Methodology: A.P., L.P., S.D., S.M.; Validation: D.C.; Investigation: A.P., G.G.; Resources: A.M.V., L.P., S.M., A.F.; Data Curation: F.C., F.R.; Writing–Original Draft Preparation: F.R., A.M.V.; Writing–Review & Editing, F.B., A.J.L.M. and E.C.deM.; Supervision: A.J.L.M. and E.C.deM.

**Funding:** A.J.L.M., and E.C.deM. were partially supported by IMET. This work was done under the agreement between IEMEST (Italy) and IMET (USA) (this is IMET contribution number IMET 19-016).

**Conflicts of Interest:** The authors declare no conflict of interest.

## References

1. La Vecchia, C.; Malvezzi, M.; Bosetti, C.; Garavello, W.; Bertuccio, P.; Levi, F.; Negri, E. Thyroid cancer mortality and incidence: A global overview. *Int. J. Cancer* **2015**, *136*, 2187–2195. [[CrossRef](#)]
2. Kondo, T.; Ezzat, S.; Asa, S.L. Pathogenetic mechanisms in thyroid follicular-cell neoplasia. *Nat. Rev. Cancer* **2006**, *6*, 292–306. [[CrossRef](#)]
3. DeGroot, L.J. Morbidity and mortality in follicular thyroid cancer. *J. Clin. Endocrinol. Metab.* **1995**, *80*, 2946–2953.
4. McHenry, C.R.; Phitayakorn, R. Follicular Adenoma and Carcinoma of the Thyroid Gland. *Oncologist* **2011**, *16*, 585–593. [[CrossRef](#)]
5. Bartolazzi, A.; Gasbarri, A.; Papotti, M.; Bussolati, G.; Lucante, T.; Khan, A.; Inohara, H.; Marandino, F.; Orlandi, F.; Nardi, F.; et al. Application of an immunodiagnostic method for improving preoperative diagnosis of nodular thyroid lesions. *Lancet* **2001**, *357*, 1644–1650. [[CrossRef](#)]
6. Macario, A.J.L.; Conway de Macario, E. Chaperone proteins and chaperonopathies. In *Stress Physiology, Biochemistry, and Pathology*; Handbook of Stress; Fink, G., Ed.; Elsevier: Amsterdam, The Netherlands; Academic Press: Cambridge, MA, USA, 2019; Volume 3, pp. 135–152.
7. Macario, A.J.L.; Conway de Macario, E.; Cappello, F. *The Chaperonopathies. Diseases with Defective Molecular Chaperones*; Springer: Dordrecht, The Netherlands; Heidelberg, Germany; New York, NY, USA; London, UK, 2013.
8. Finka, A.; Sharma, S.K.; Goloubinoff, P. Multi-layered molecular mechanisms of polypeptide holding, unfolding and disaggregation by HSP70/HSP110 chaperones. *Front. Mol. Biosci.* **2015**, *2*, 29. [[CrossRef](#)] [[PubMed](#)]
9. Mogk, A.; Bukau, B.; Kampinga, H.H. Cellular Handling of Protein Aggregates by Disaggregation Machines. *Mol. Cell* **2018**, *69*, 214–226. [[CrossRef](#)] [[PubMed](#)]
10. Willison, K.R. The structure and evolution of eukaryotic chaperonin-containing TCP-1 and its mechanism that folds actin into a protein spring. *Biochem. J.* **2018**, *475*, 3009–3034. [[CrossRef](#)] [[PubMed](#)]
11. Adams, B.M.; Oster, M.E.; Hebert, D.N. Protein Quality Control in the Endoplasmic Reticulum. *Protein J.* **2019**, *38*, 317–329. [[CrossRef](#)]
12. Dahiya, V.; Buchner, J. Functional principles and regulation of molecular chaperones. *Insights Enzym. Mech. Funct. Exp. Comput. Methods* **2019**, *114*, 1–60.
13. Kampinga, H.H.; Hageman, J.; Vos, M.J.; Kubota, H.; Tanguay, R.M.; Bruford, E.A.; Cheetham, M.E.; Chen, B.; Hightower, L.E. Guidelines for the nomenclature of the human heat shock proteins. *Cell Stress Chaperones* **2009**, *14*, 105–111. [[CrossRef](#)]
14. Macario, A.J.L.; Conway de Macario, E. Sick Chaperones, Cellular Stress, and Disease. *N. Engl. J. Med.* **2005**, *353*, 1489–1501. [[CrossRef](#)] [[PubMed](#)]
15. Rappa, F.; Sciume, C.; Bello, M.L.; Bavisotto, C.C.; Gammazza, A.M.; Barone, R.; Campanella, C.; David, S.; Carini, F.; Zarcone, F.; et al. Comparative analysis of Hsp10 and Hsp90 expression in healthy mucosa and adenocarcinoma of the large bowel. *Anticancer Res.* **2014**, *34*, 4153–4159.
16. Chatterjee, S.; Burns, T.F. Targeting Heat Shock Proteins in Cancer: A Promising Therapeutic Approach. *Int. J. Mol. Sci.* **2017**, *18*, 1978. [[CrossRef](#)] [[PubMed](#)]

17. Mineva, I.; Gärtner, W.; Hauser, P.; Kainz, A.; Löffler, M.; Wolf, G.; Oberbauer, R.; Weissel, M.; Wagner, L. Differential expression of alphaB-crystallin and Hsp27-1 in anaplastic thyroid carcinomas because of tumor-specific alphaB-crystallin gene (CRYAB) silencing. *Cell Stress Chaperones* **2005**, *10*, 171–184. [[CrossRef](#)] [[PubMed](#)]
18. Mo, X.-M.; Li, L.; Zhu, P.; Dai, Y.-J.; Zhao, T.-T.; Liao, L.-Y.; Chen, G.G.; Liu, Z.-M. Up-regulation of Hsp27 by ER $\alpha$ /Sp1 facilitates proliferation and confers resistance to apoptosis in human papillary thyroid cancer cells. *Mol. Cell. Endocrinol.* **2016**, *431*, 71–87. [[CrossRef](#)]
19. Rappa, F.; Farina, F.; Zummo, G.; David, S.; Campanella, C.; Carini, F.; Tomasello, G.; Damiani, P.; Cappello, F.; Conway de Macario, E.; et al. HSP-molecular chaperones in cancer biogenesis and tumor therapy: An overview. *Anticancer Res.* **2012**, *32*, 5139–5150.
20. Walsh, D.; Grantham, J.; Zhu, X.O.; Lin, J.W.; Van Oosterum, M.; Taylor, R.; Edwards, M. The role of heat shock proteins in mammalian differentiation and development. *Environ. Med.* **1999**, *43*, 79–87.
21. Barna, J.; Csermely, P.; Vellai, T. Roles of heat shock factor 1 beyond the heat shock response. *Cell. Mol. Life Sci.* **2018**, *75*, 2897–2916. [[CrossRef](#)]
22. Park, A.-M.; Kanai, K.; Itoh, T.; Sato, T.; Tsukui, T.; Inagaki, Y.; Selman, M.; Matsushima, K.; Yoshie, O. Heat Shock Protein 27 Plays a Pivotal Role in Myofibroblast Differentiation and in the Development of Bleomycin-Induced Pulmonary Fibrosis. *PLoS ONE* **2016**, *11*, e0148998. [[CrossRef](#)]
23. Hance, M.W.; Dole, K.; Gopal, U.; Bohonowych, J.E.; Jezierska-Drutel, A.; Neumann, C.A.; Liu, H.; Garraway, I.P.; Isaacs, J.S. Secreted Hsp90 Is a Novel Regulator of the Epithelial to Mesenchymal Transition (EMT) in Prostate Cancer. *J. Biol. Chem.* **2012**, *287*, 37732–37744. [[CrossRef](#)]
24. Rappa, F.; Pitruzzella, A.; Marino Gammazza, A.; Barone, R.; Mocciano, E.; Tomasello, G.; Carini, F.; Farina, F.; Zummo, G.; Conway de Macario, E.; et al. Quantitative patterns of Hsps in tubular adenoma compared with normal and tumor tissues reveal the value of Hsp10 and Hsp60 in early diagnosis of large bowel cancer. *Cell Stress Chaperones* **2016**, *21*, 927–933. [[CrossRef](#)]
25. Li, X.-S.; Xu, Q.; Fu, X.-Y.; Luo, W.-S. Heat Shock Protein 60 Overexpression Is Associated with the Progression and Prognosis in Gastric Cancer. *PLoS ONE* **2014**, *9*, e107507. [[CrossRef](#)]
26. Lianos, G.D.; Alexiou, G.A.; Mangano, A.; Mangano, A.; Rausei, S.; Boni, L.; Dionigi, G.; Roukos, D.H.; Dionigi, M.P.G. The role of heat shock proteins in cancer. *Cancer Lett.* **2015**, *360*, 114–118. [[CrossRef](#)]
27. Wu, J.; Liu, T.; Rios, Z.; Mei, Q.; Lin, X.; Cao, S. Heat Shock Proteins and Cancer. *Trends Pharm. Sci* **2017**, *38*, 226–256. [[CrossRef](#)]
28. Vidyasagar, A.; Wilson, N.A.; Djamali, A. Heat shock protein 27 (HSP27): Biomarker of disease and therapeutic target. *Fibrogenes. Tissue Repair* **2012**, *5*, 7. [[CrossRef](#)]
29. Concannon, C.G.; Gorman, A.; Samali, A. On the role of Hsp27 in regulating apoptosis. *Apoptosis* **2003**, *8*, 61–70. [[CrossRef](#)]
30. Zheng, G.; Zhang, Z.; Liu, H.; Xiong, Y.; Luo, L.; Jia, X.; Peng, C.; Zhang, Q.; Li, N.; Gu, Y.; et al. HSP27-Mediated Extracellular and Intracellular Signaling Pathways Synergistically Confer Chemoresistance in Squamous Cell Carcinoma of Tongue. *Clin. Cancer Res.* **2018**, *24*, 1163–1175. [[CrossRef](#)]
31. Sheng, B.; Qi, C.; Liu, B.; Lin, Y.; Fu, T.; Zeng, Q. Increased HSP27 correlates with malignant biological behavior of non-small cell lung cancer and predicts patient's survival. *Sci. Rep.* **2017**, *7*, 13807. [[CrossRef](#)]
32. Keezer, S.M.; Ivie, S.E.; Krutzsch, H.C.; Tandle, A.; Libutti, S.K.; Roberts, D.D. Angiogenesis inhibitors target the endothelial cell cytoskeleton through altered regulation of heat-shock protein 27 and cofilin. *Cancer Res.* **2003**, *63*, 6405–6412.
33. Cappello, F.; Marino Gammazza, A.; Palumbo Piccionello, A.; Campanella, C.; Pace, A.; Conway de Macario, E.; Macario, A.J.L. Hsp60 chaperonopathies and chaperonotherapy: Targets and agents. *Expert Opin. Ther. Targets* **2014**, *18*, 185–208. [[CrossRef](#)]
34. Martorana, G.; Belfiore, P.; Martorana, A.; Bucchieri, F.; Cappello, F.; Bellafiore, M.; Palma, A.; Marciano, V.; Farina, F.; Zummo, G. Expression of 60-kD Heat Shock Protein Increases during Carcinogenesis in the Uterine Exocervix. *Pathobiology* **2002**, *70*, 83–88.
35. Cappello, F.; Bellafiore, M.; Palma, A.; David, S.; Marcianò, V.; Bartolotta, T.; Sciumè, C.; Modica, G.; Farina, F.; Zummo, G.; et al. 60KDa chaperonin (HSP60) is over-expressed during colorectal carcinogenesis. *Eur. J. Histochem.* **2003**, *47*, 105–110. [[CrossRef](#)]
36. Rérole, A.-L.; Jego, G.; Garrido, C. Hsp70: Anti-apoptotic and Tumorigenic Protein. *Adv. Struct. Saf. Stud.* **2011**, *787*, 205–230.

37. Ciocca, D.R.; Calderwood, S.K. Heat-shock proteins in cancer: Diagnostic, prognostic, predictive, and treatment implications. *Cell Stress Chaperones* **2005**, *10*, 86–103. [[CrossRef](#)]
38. Burrows, F.; Zhang, H.; Kamal, A. Hsp90 Activation and Cell Cycle Regulation. *Cell Cycle* **2004**, *3*, 1530–1536. [[CrossRef](#)]
39. Sun, J.; Liao, J.K. Induction of angiogenesis by heat-shock protein 90 mediated by protein kinase Akt and endothelial nitric oxide synthase. *Atheroscler. Thromb. Vasc. Biol.* **2004**, *24*, 2238–2244. [[CrossRef](#)]
40. Feron, O.; Pfosser, A.; Thalgott, M.; Büttner, K.; Brouet, A.; Boekstegers, P.; Kupatt, C. Liposomal Hsp90 cDNA induces neovascularization via nitric oxide in chronic ischemia. *Cardiovasc. Res.* **2005**, *65*, 728–736.
41. Bryantsev, A.L.; Chechenova, M.B.; Shelden, E.A. Recruitment of phosphorylated small heat shock protein Hsp27 to nuclear speckles without stress. *Exp. Cell Res.* **2007**, *313*, 195–209. [[CrossRef](#)]
42. Baker-Williams, A.J.; Hashmi, F.; Budzyński, M.A.; Woodford, M.R.; Gleicher, S.; Himanen, S.V.; Makedon, A.M.; Friedman, D.; Cortes, S.; Namek, S.; et al. Co-chaperones TIMP2 and AHA1 Competitively Regulate Extracellular HSP90:Client MMP2 Activity and Matrix Proteolysis. *Cell Rep.* **2019**, *28*, 1894–1906. [[CrossRef](#)]
43. Xiang, L.; Gilkes, D.M.; Chaturvedi, P.; Luo, W.; Hu, H.; Takano, N.; Liang, H.; Semenza, G.L. Ganetespib blocks HIF-1 activity and inhibits tumor growth, vascularization, stem cell maintenance, invasion, and metastasis in orthotopic mouse models of triple-negative breast cancer. *J. Mol. Med.* **2014**, *92*, 151–164. [[CrossRef](#)]



© 2019 by the authors. Licensee MDPI, Basel, Switzerland. This article is an open access article distributed under the terms and conditions of the Creative Commons Attribution (CC BY) license (<http://creativecommons.org/licenses/by/4.0/>).